Supporting Information

Simultaneous imaging of mitochondrial viscosity and hydrogen peroxide in Alzheimer's disease by a single near-infrared fluorescent probe with large Stokes shift

Songjiao Li, Peipei Wang, Wenqi Feng, Yunhui Xiang, Kun Dou, Zhihong Liu*,†

†Key Laboratory of Analytical Chemistry for Biology and Medicine (Ministry of Education), College of Chemistry and Molecular Sciences, Wuhan University, Wuhan, Hubei 430072, China.

*Corresponding Author.

Zhihong Liu. E-mail: zhhliu@whu.edu.cn.

Phone: 86-27-8721-7886. Fax: 86-27-6875-4067.

Table of contents

EXPERIMENTAL SECTION

Materials and apparatus

All commercially available reagents were used as provided without further purifications. Chemicals and solvents were purchased from the companies Sigma Aldrich, Aladdin, Bepharm, etc. All aqueous solutions were prepared by using ultrapure water with a resistivity of 18.25 MΩ (purified by Milli-Q system supplied by Millipore). The pH of the buffer solution was controlled by a digital pH meter (FE20, MettlerToledo). High-resolution mass spectra (HRMS) were obtained from DIONEX UltiMate 3000 & Bruker Compact TOF mass spectrometer. NMR spectra were recorded on a Bruker AVANCE III HD spectrometer, using TMS as an internal standard; Absorption spectra were measured on a Shimadzu UV 2550 UV-Vis spectrophotometer. The fluorescence spectra were measured on a Shimadzu RF-6000 fluorophotometer. The fluorescence microscopy images of HeLa cells were acquired by PerkinElmer UltraVIEW VoX. The viscosity was measured with a NDJ-8S rotational viscometer (China).

Synthesis and Characterization

Synthesis. The synthetic route for compound Mito-NIRHV from commercially available materials is depicted in Scheme S1.

Compound 1: 4-bromo-N, N-dimethylaniline (1 g, 5 mmol) and $Pd(PPh_3)_4$ (0.49 g, 0.43 mmol) were dissolved in 15 mL of THF under argon. Then K_2CO_3 aqueous solution (2 M, 1.25 mL) was added. After 1 hour, 5-formyl-2-thiophene boronic acid (1.6 g, 10 mmol) dissolved in 10 mL of THF was slowly added to the reaction solution and the reaction mixture was stirred at 80 °C for 12 hours. After the reaction was completed, the reaction mixture was cooled to room temperature and poured into saturated NaCl solution and extracted with CH_2Cl_2 (50 mL × 3). The organic layer was then dried over Na_2SO_4 and concentrated under vacuum, and then the crude

product was purified by silica gel chromatography using dichloromethane/petroleum ether (v/v, 2:1) as the eluent to afford compound 1 as a yellow solid (340 mg): Yield 30%. ^{1}H NMR (400 MHz, $CDCl_3$, Figure S1) δ 9.74 (s 1H), 7.61 (d, J = 4.0 Hz, 1H), 7.50 (d, J = 8.0 Hz, 1H), 7.18 (d, J = 4.0 Hz, 1H), 6.66 (d, J = 12.0 Hz, 1H), 2.95 (s, 6H). ^{13}C NMR (101 MHz, $CDCl_3$, Figure S2) δ 182.5, 156.1, 151.1, 140.1, 138.2, 127.5, 121.5, 112.1, 40.3. HRMS (Figure S3) m/z: calcd for $C_{13}H_{13}NOS$ $[M+H]^+$: 231.072 found: 231.079.

Compound 2: 4-Methylchinoline (0.6 g, 4.2 mmol) and 4-(bromomethyl)-benzeneboronic acid pinacol ester (1.8 g, 6.3 mmol) were dissolved in toluene, and then the mixture was refluxed at 110 °C for 12 h. The obtained grey powdery solid was filtered, washed with toluene, and dried in vacuo to afford pure compound 2 (1.2 g): Yield 65%. ^{1}H NMR (400 MHz, CD_3CN, Figure S4) δ 9.35 (d, J = 4.0 Hz, 1H), 8.50 (dd, J = 8.0 Hz, 1H), 8.30 (d, J = 8.0 Hz, 1H), 8.11-8.07 (m, 1H), 7.99-7.95 (m, 2H), 7.72 (d, J = 8.0 Hz, 2H), 7.31 (d, J = 8.0 Hz, 2H), 6.26 (s, 2H), 3.04 (s, 3H), 1.30 (s, 12H). ^{13}C NMR (101 MHz, CD_3CN, Figure S5) δ 161.2, 149.1, 136.9, 136.0, 135.7, 130.4, 129.5, 128.8, 127.8, 127.3, 123.4, 120.0, 84.7, 60.9, 24.7, 20.2. HRMS (Figure S6) m/z: calcd for $C_{23}H_{27}BNO_2$ $[M]^+$: 360.213 found: 360.214.

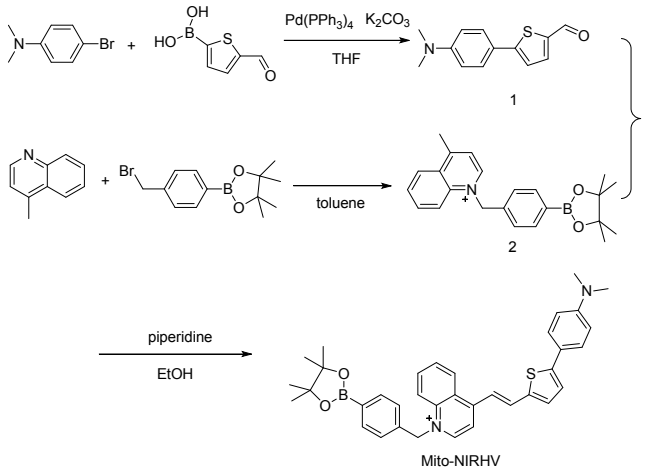

Scheme S1. Synthetic Route for Mito-NIRHV.

Probe Mito-NIRHV: Compound 1 (0.23 g, 1 mmol) and compound 2 (0.36 g, 1 mmol) were mixed in ethanol (20 mL), and then piperidine (0.05 mL) was added to the solution. The reaction mixture was refluxed with stirring for 4 h and then evaporated

in vacuo. The organic layer was then dried over Na_2SO_4 and concentrated under vacuum, and then the crude product was purified by silica gel chromatography using CH_2Cl_2/MeOH (v/v, 10:1) as the eluent to yield Mito-NIRHV as a blue solid (19.5 mg): Yield 30%. ^{1}H NMR (400 MHz, CD_3OD, Figure S7) δ 9.12 (d, J = 8.0 Hz, 1H), 8.74 (d, J = 8.0 Hz, 1H), 8.31-8.28 (m, 2H), 8.06-8.01 (m, 2H), 7.92 (t, J = 8.0 Hz, 1H), 7.73 (d, J = 12.0 Hz, 2H), 7.55-7.51 (m, 4H), 7.30-7.26 (m, 3H), 6.72 (d, J = 8.0 Hz, 2H), 6.11 (s, 2H), 3.00 (s, 6H), 1.31 (s, 6H), 1.28 (s, 6H). ^{13}C NMR (101 MHz, CD_3OD, Figure S8) δ 160.5, 148.4, 146.4, 141.1, 140.8, 137.6, 135.4, 135.2, 134.9, 134.7, 134.6, 129.8, 129.7, 127.0, 126.7, 126.0, 125.9, 122.6, 119.4, 84.3, 60.4, 39.0, 19.1. HRMS (Figure S9) m/z: calcd for $C_{36}H_{38}BN_2O_2S$ $[M]^+$: 573.274 found: 573.272.

Preparation of ROS/RNS

H_2O_2 was generated by dilution of a 30% solution in deionized water. ClO^- was generated by dilution of a 5% NaClO solution in deionized water. Hydroxyl radicals (•OH) were generated by the Fenton reaction. For this purpose, hydrogen peroxide (H_2O_2, 100 μM) was added to a solution of ammonium iron (II) sulfate (100 μM) in deionized water. Singlet oxygen ($^1O_2$) was generated in situ by addition of a H_2O_2 stock to a solution containing 10 equiv of HClO. Superoxide solution ($O_2^{\bullet-}$) was prepared by adding KO_2 to dry DMSO and stirring vigorously for 10 min. Nitric oxide (NO) was used from a stock solution prepared from DEA·NONOate. Peroxynitrite ($ONOO^-$) solution was prepared as follows a mixture of sodium nitrite (0.6 M) and hydrogen peroxide (0.7 M) was acidified with hydrochloric acid (0.6 M), and sodium hydroxide (1.5 M) was added within 1-2 s to make the solution alkaline. The $ONOO^-$ concentration was estimated using an extinction coefficient of 1670 $M^{-1}cm^{-1}$ at 302 nm. Stock solutions (1.0 mM) of Cys, GSH, Hcy were prepared in ultrapure water.

General Procedures for Analysis

A parent stock solution of probe Mito-NIRHV (1.0 mM) was prepared in dimethyl sulfoxide (DMSO). The working standards were prepared by placing 10 μL of the parent stock solution and the appropriate volume of the other solution into a test tube and then diluting the solution to 1 mL with DMSO/PBS (3:7, v/v, PBS, 10 mM, pH 7.4). The solutions were measured in a UV spectrophotometer and a fluorescence spectrophotometer.

Viscosity determination and fluorescence measurements

The solvents were obtained by mixing an ethanol-glycerol system in different proportions. Measurements were carried out with an NDJ-8S rotational viscometer, and each viscosity value was recorded. The solutions of Mito-NIRHV of different viscosity were prepared by adding the stock solution (1.0 mM) 10 μL to 1 mL of solvent mixture (ethanol-glycerol solvent systems) to obtain the final concentration of Mito-NIRHV (10.0 μM). These solutions were sonicated for 5 minutes to eliminate air bubbles. After standing for 1 hour at a constant temperature, the solutions were measured in a UV spectrophotometer and a fluorescence spectrophotometer.

The measurement of lipophilicity (Log P)

Lipophilicity was presented as log $P_{o/w}$ values, which were determined by the flask-shaking method. To evaluate Log P of the Mito-NIRHV, solution of the probes (30 μM) were partitioned in a mixture of octanol (0.5 mL) and water (0.5 mL). After vortexing, the mixture was centrifuged at 2000 rpm for 5 min. The octanol layer was separated from the water layer and the absorbance of both layers was measured by a Shimadzu UV 2550 UV-Vis spectrophotometer. Log P was defined as the logarithmic ratio of probe concentrations in the organic and aqueous phase.

Cytotoxicity assays

The cytotoxicity was evaluated by MTT assay. HeLa cells were cultured in Dulbecco's modified Eagle's medium (DMEM) in 96-well microplates at 37 °C under 5% CO_2 for 12 h. The medium was next replaced by fresh medium containing various concentrations of Mito-NIRHV (0-40 μM/mL). Each concentration was tested in three replicates. Cells were rinsed twice with phosphate buffer saline 24 h later and incubated with 0.5 mg/mL MTT reagent for 4 h at 37 °C. 100 μL of DMSO was then added to dissolve formazan. The absorbance at 490 nm was measured in a microplate reader. Cell viability (%) was calculated according to following equation: Viability = (mean Abs. of treated wells/mean Abs. of control wells) ×100%.

Cell imaging

The living HeLa cells were cultured in DMEM (Dulbecco's modified Eagle's medium) supplemented with 10% FBS (fetal bovine serum) at 37 °C in a 5% CO_2 atmosphere.

1) Imaging of H_2O_2 in living cells

Five groups of cells were treated differently and imaged. The first group of cells were incubated with Mito-NIRHV (10 μM) at 37 °C for 30 min. The second group of cells were treated with H_2O_2 (50 μM) at 37 °C for 30 min, then incubated with Mito-NIRHV (10 μM) for another 30 min. The third group of cells were treated with H_2O_2 (100 μM) at 37 °C for 30 min, then incubated with Mito-NIRHV (10 μM) for another 30 min. The fourth group of cells were treated with PMA (1 μg/mL) at 37 °C for 30 min, then incubated with Mito-NIRHV (10 μM) for another 30 min. The last group of cells were incubated with NAC (1 mM) for 30 min prior to the PMA (1 μg/mL) stimulation, then incubated with Mito-NIRHV (10 μM) for another 30 min. Prior to the imaging, the cells were washed three times with PBS, and the fluorescence images were acquired through PerkinElmer UltraVIEW VoX with excitation wavelength at 488 nm and emission wavelength at 668-726 nm.

2) Imaging of viscosity in living cells

HeLa cells was incubated with ionophores (monensin and nystatin) (10 μM) for 30 min at 37 °C and then washed with PBS twice, and the cells were incubated with Mito-NIRHV (10 μM) for 30 min at 37 °C, and then washed with PBS three times, and the fluorescence images were acquired through a PerkinElmer UltraVIEW VoX with excitation wavelength at 561 nm and emission wavelength at 754-816 nm.

3) Simultaneous imaging of H_2O_2 and viscosity in living cells.

For the detection of H_2O_2 and viscosity, the HeLa cells were incubated with 100 μg/mL LPS for 6 h, then incubated with Mito-NIRHV (10 μM) for another 30 min. Prior to the imaging, the cells were washed three times with PBS, and the fluorescence images were acquired through a PerkinElmer UltraVIEW VoX. The excitation wavelengths were 488 and 561 nm, and collection windows were at 668-726 nm and 754-816 nm, respectively.

Living mice Imaging.

Male balb/c mice (weight 20 ± 2 g) were supplied from Wuhan Center for Disease Control and Prevention. All animal studies were performed in accordance with Animal Care and Use Committee of Wuhan University. All groups contained three mice.

1) Imaging of H_2O_2 in living mice.

The mice were divided into three groups and treated differently. The first group of mice was given an intraperitoneal injection of Mito-NIRHV (1 mM, 100 μL). The second group of mice was i.p. injected with H_2O_2 (1 mM in saline, 100 μL) for 30 min, followed by i.p. injection with Mito-NIRHV (1 mM, 100 μL). The third group of mice was given an injection of rotenone (1 mM, 100 μL) into the peritoneal cavity followed by injection of Mito-NIRHV (1 mM, 100 μL) at the same region after 1 h. After 30 min, mice were anesthetized using isoflurane and imaged with an IVIS imaging system (λ_{ex} = 430 nm, λ_{em} = 700 nm).

2) Imaging of viscosity in living mice.

These mice were injected by monensin, nystatin in abdomen respectively to produce viscosity increasing models. After 4 h, the triggered mice and normal mice were simultaneously utilized for in vivo imaging. Mito-NIRHV (1 mM, 100 μL) was then injected into the abdominal position of the normal mice and triggered mice, respectively. After 30 min, mice were anesthetized using isoflurane and imaged with an IVIS imaging system (λ_{ex} = 570 nm, λ_{em} = 800 nm).

3) Simultaneous imaging of H_2O_2 and viscosity in living mice.

The mice were given an i.p. injection of LPS (400 μL, 1 mg/mL). After 4 h, the mice were injected i.p. with Mito-NIRHV (1 mM, 100 μL). As a control, unstimulated mice i.p. injected only with Mito-NIRHV (1 mM, 100 μL) were also prepared. The mice were then imaged (30 min after the injection of Mito-NIRHV) by using an IVIS imaging system. Channel 1: λ_{ex} = 430 nm, λ_{em} = 700 nm; Channel 2: λ_{ex} = 570 nm, λ_{em} = 800 nm.

4) Assessment on BBB Penetration.

BALB/c mice were i.v. injected with Mito-NIRHV (2.0 mg/kg). After 30 min, mice were perfused with saline solution, and the brains were harvested. The brain samples were homogenized in 2.0 mL water followed by the addition of ethyl acetate (2.0 mL). The resulting homogenate was stirred for 2 h and centrifuged for 5 min at 3750 × g. The extractions were subjected to HRMS analysis.

5) Whole-Brain NIRF Imaging of H_2O_2 and viscosity in AD mice.

The IVIS Spectrum animal imaging system (PerkinElmer) was used to perform In vivo NIR imaging. Images were acquired with Channel 1: λ_{ex} = 430 nm, λ_{em} = 700 nm; Channel 2: λ_{ex} = 570 nm, λ_{em} = 800 nm. Living Image 4.5 software (PerkinElmer) was used for data analysis. Mice (n = 3 male transgenic APP-PS1 mice and n = 3 age matched male wild-type control mice) were shaved before background imaging and were i.v. injected with freshly prepared Mito-NIRHV (2.0 mg/kg, 30% DMSO and 70% PBS). Fluorescence signals from the brain were recorded before and 60 min after i.v. injection of the probe. To evaluate our imaging results, a region of interest (ROI) was drawn around the brain region.

6) Histological Staining of the Tissue Slices

After imaging, the mice were killed, the brains were collected for tissue analysis. Though a series of standard procedures, including fixation in 10% neutral buffered formalin, embedding into paraffin and sectioning at 3 μm thickness, the tissues were stained with hematoxylin-eosin (H&E). Thereafter, the prepared slices were examined by a digital microscope.

SUPPLEMENTAL FIGURES

Characterization of Compound 1

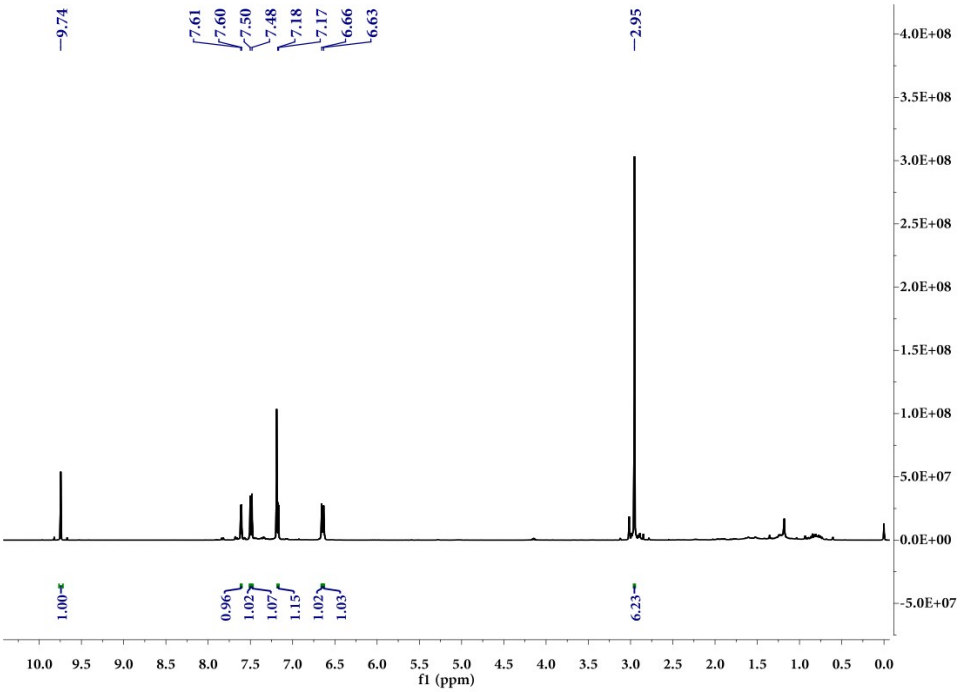

Figure S1. ^{1}H NMR spectrum of compound 1 in $CDCl_3$.

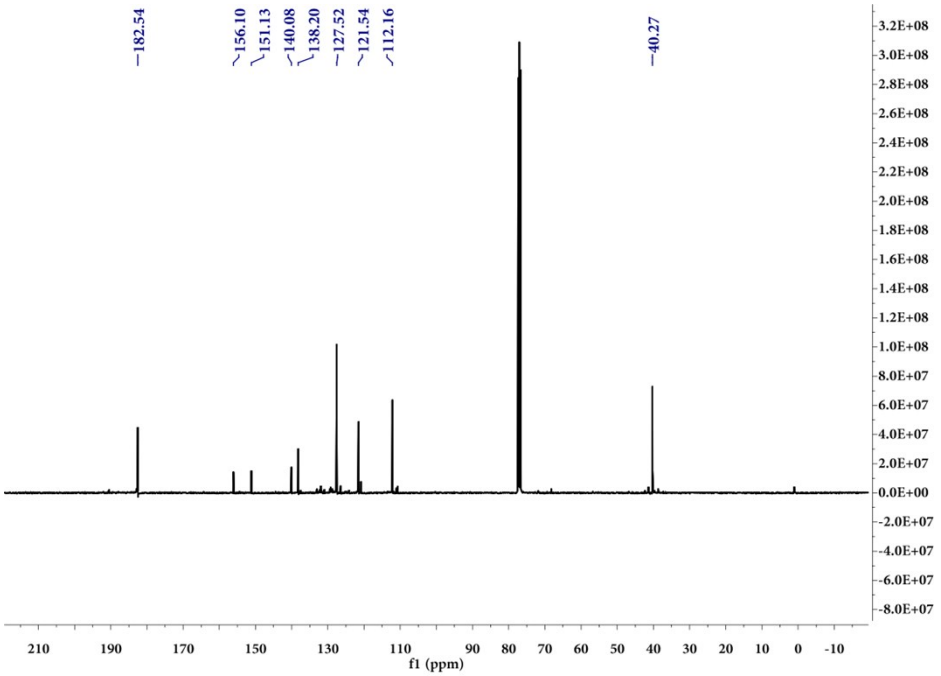

Figure S2. ^{13}C NMR spectrum of compound 1 in $CDCl_3$.

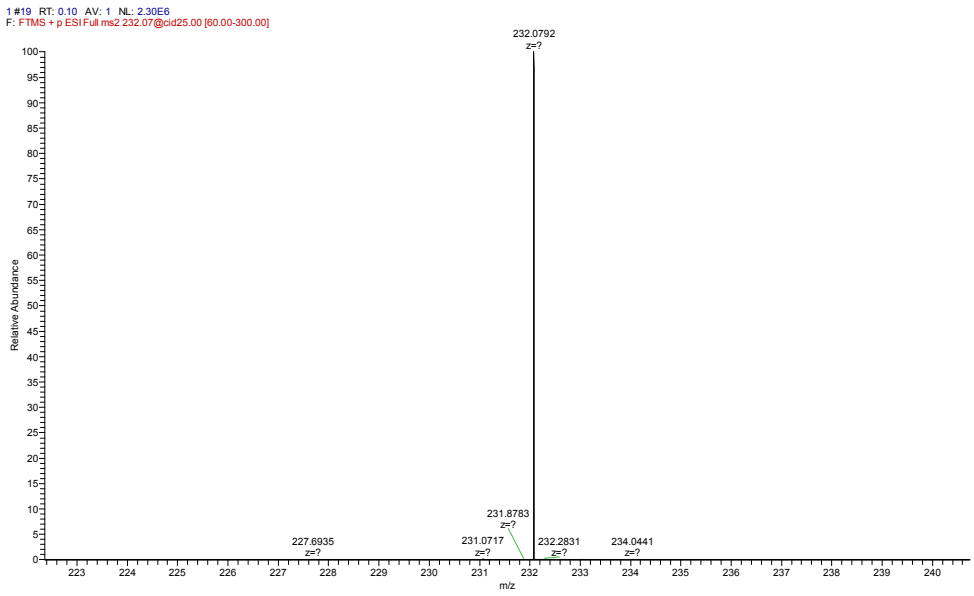

Figure S3. HRMS spectrum of compound 1.

Characterization of Compound 2

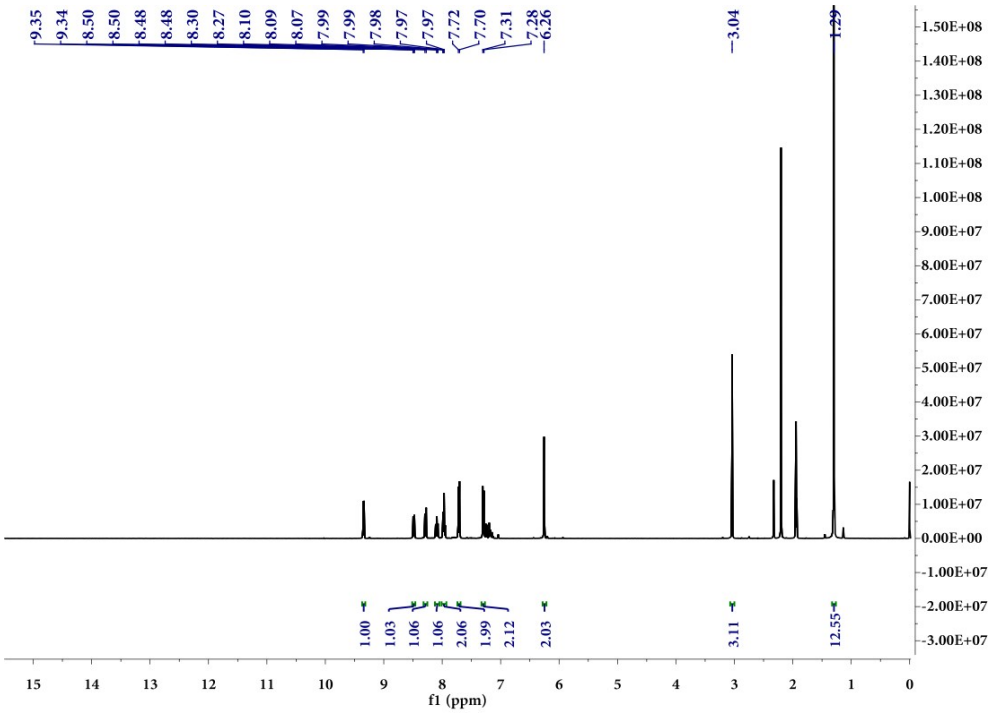

Figure S4. ^{1}H NMR spectrum of compound 2 in CD_3CN.

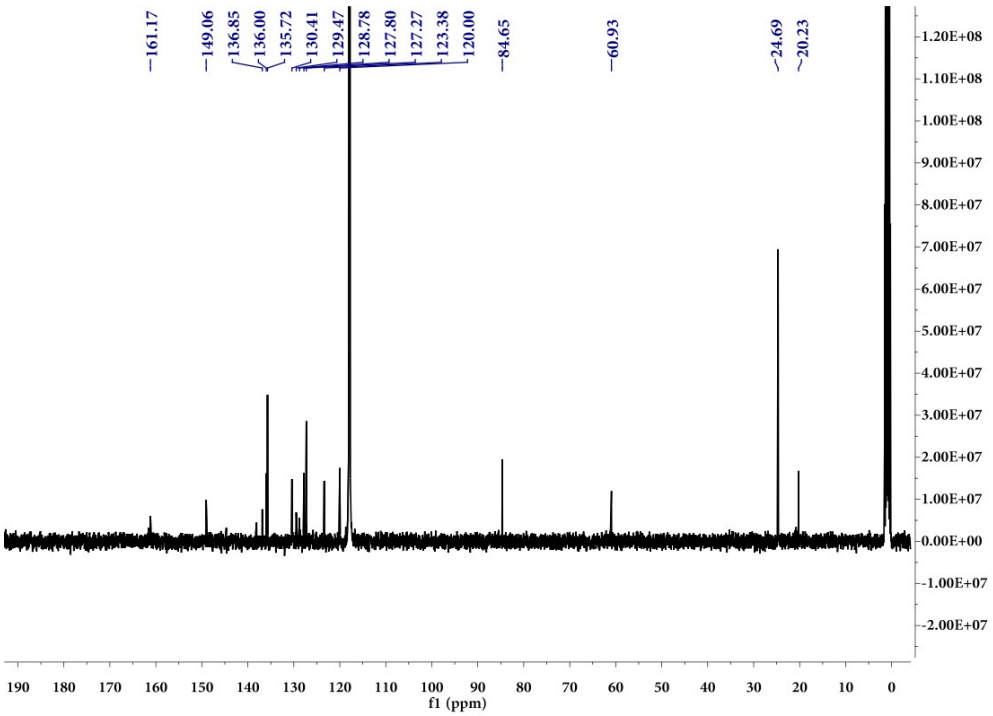

Figure S5. ^{13}C NMR spectrum of compound 2 in CD_3CN.

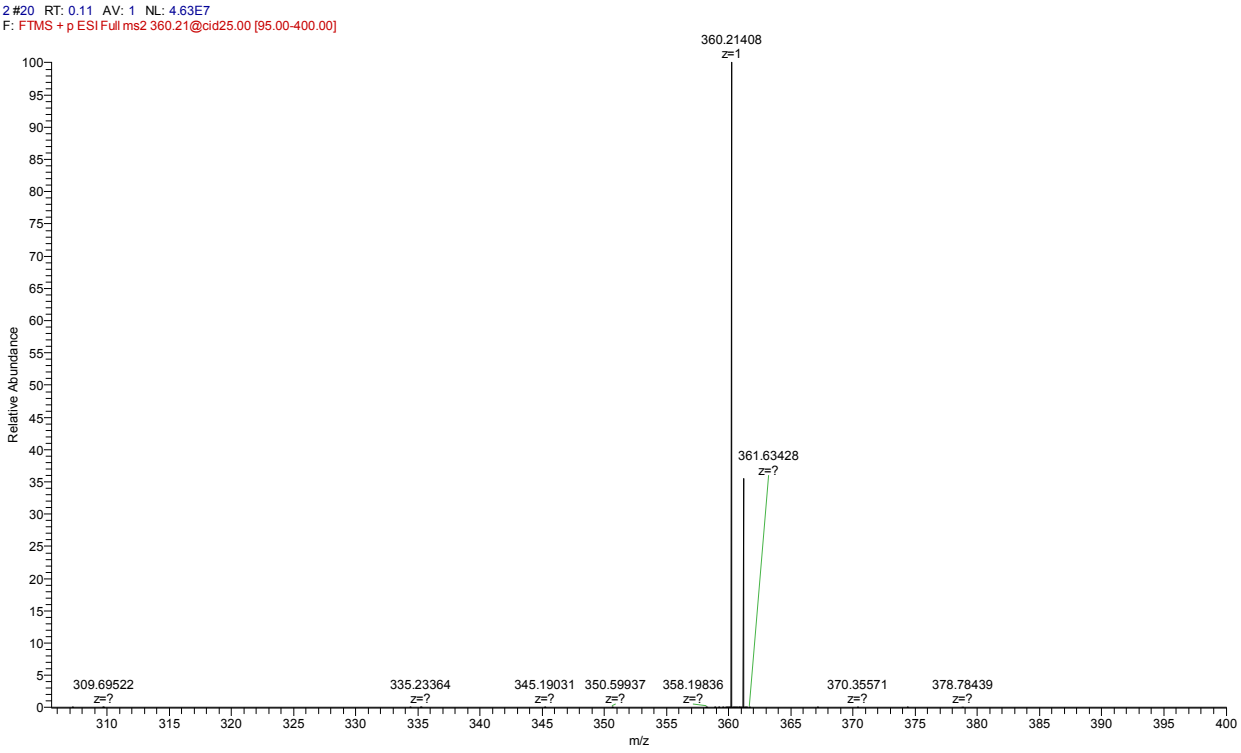

Figure S6. HRMS spectrum of compound 2.

Characterization of Mito-NIRHV

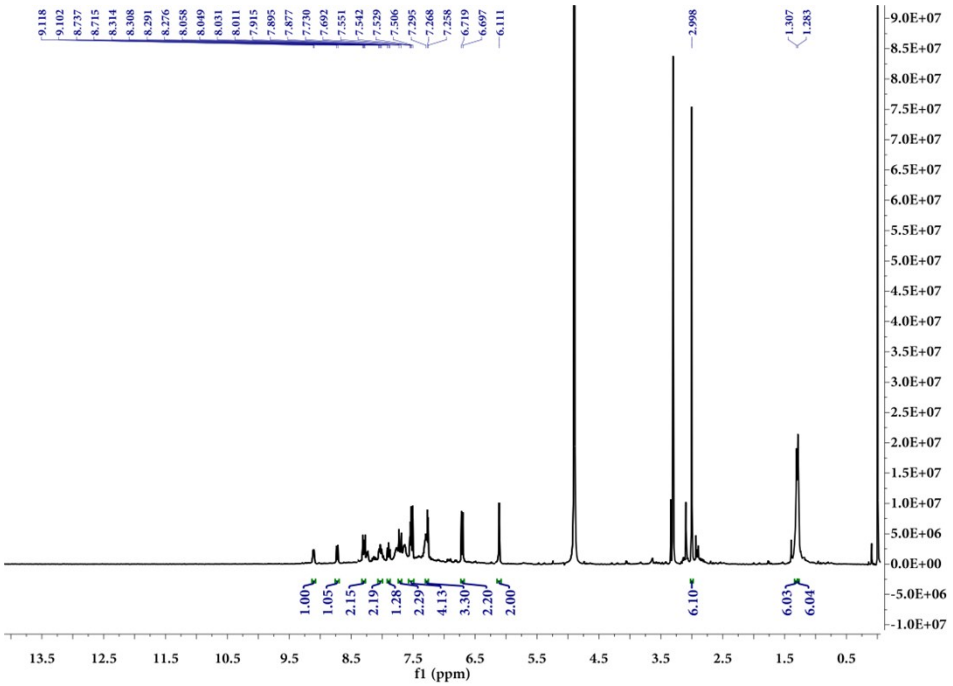

Figure S7. ^{1}H NMR spectrum of Mito-NIRHV in CD_3OD.

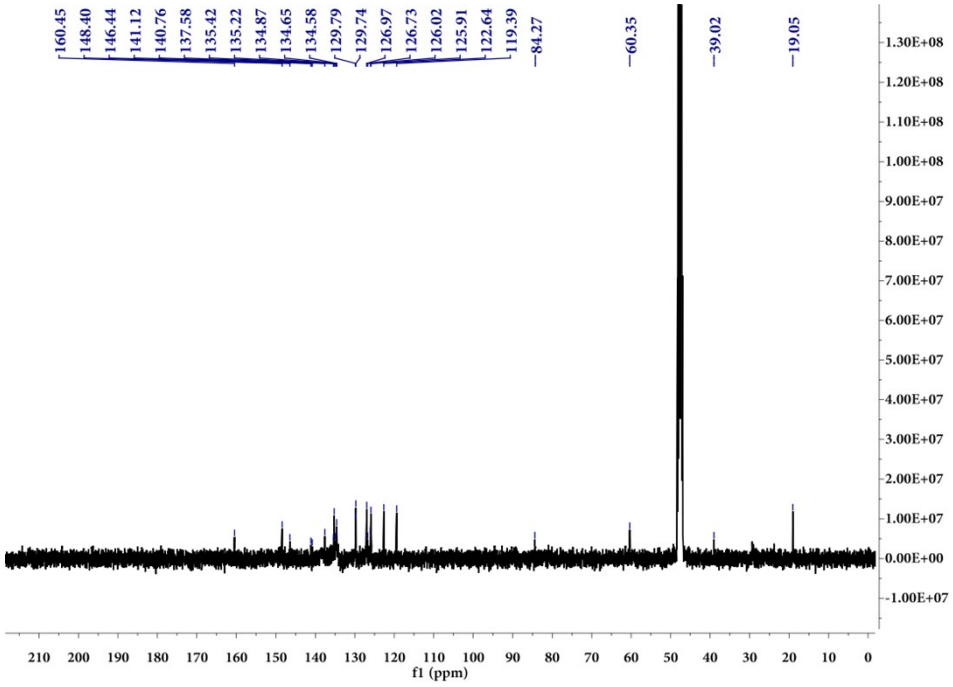

Figure S8. ^{13}C NMR spectrum of Mito-NIRHV in CD_3OD.

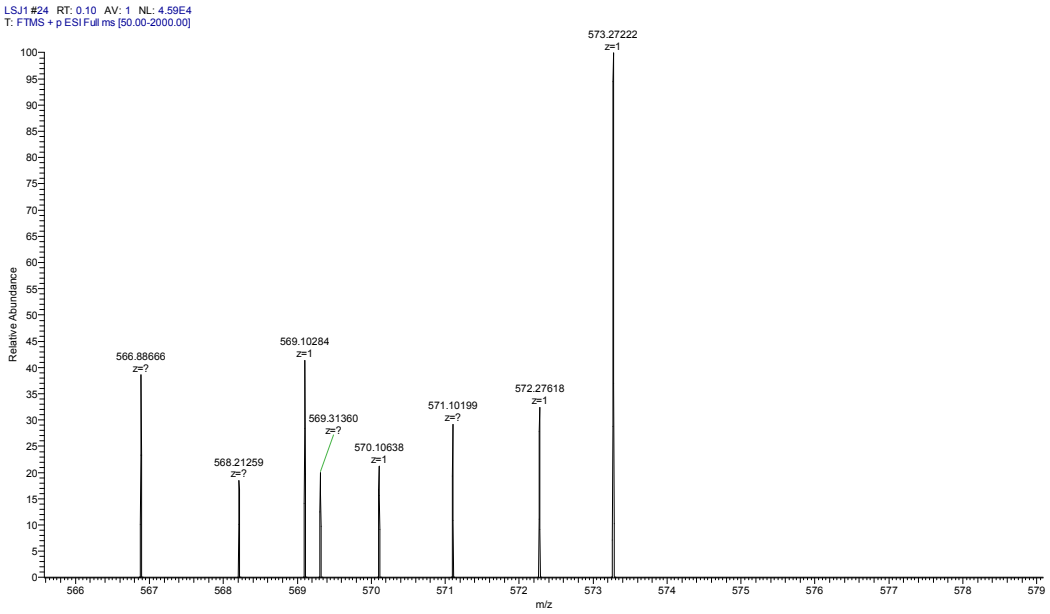

Figure S9. HRMS spectrum of Mito-NIRHV.

Response of Mito-NIRHV to H_2O_2

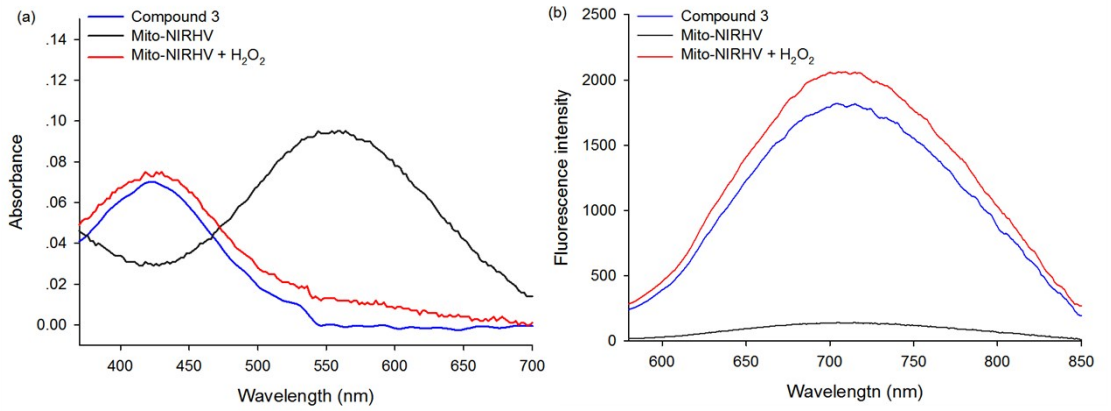

Figure S10. (a) Absorption and (b) fluorescence spectra of 10 μM Compound 3 (blue), Mito-NIRHV (10 μM) before (black) and after (red) reacting with H_2O_2 (100 μM). The measurements were performed in DMSO/PBS, 3:7 (v/v), pH 7.4, at room temperature.

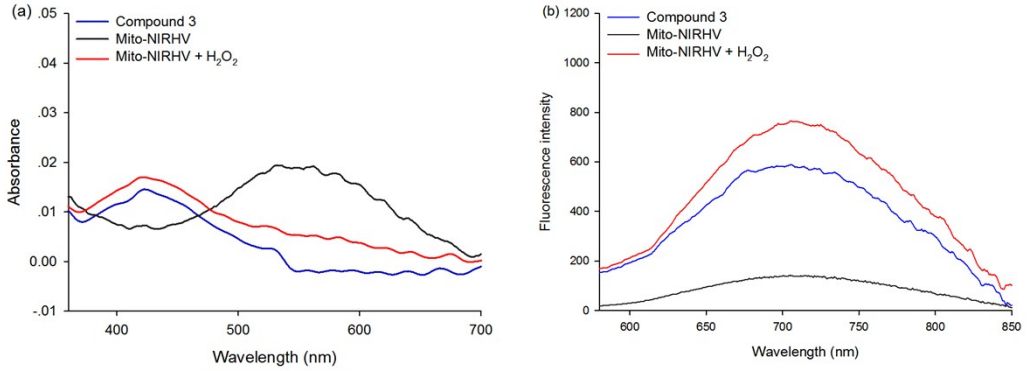

Figure S11. (a) Absorption and (b) fluorescence spectra of 2 μM Compound 3 (blue), Mito-NIRHV (2 μM) before (black) and after (red) reacting with H_2O_2 (100 μM). The measurements were performed in DMSO/PBS, 3:7 (v/v), pH 7.4, at room temperature.

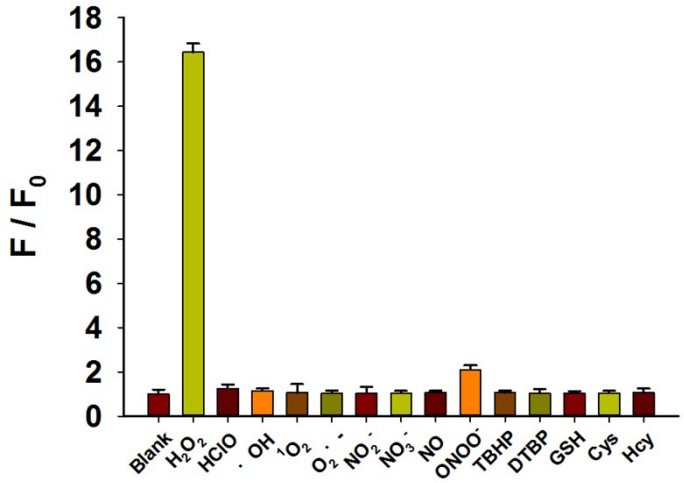

Figure S12. Fluorescence responses of Mito-NIRHV (10 μM) toward various ROS/RNS/RSS (100 μM): (1) Blank; (2) H_2O_2; (3) HClO; (4) •OH; (5) $^1O_2$; (6) $O_2^{\bullet-}$; (7) NO_2^-; (8) NO_3^-; (9) NO; (10) $ONOO^-$; (11) TBHP; (12) DTBH; (13) GSH; (14) Cys; (15) Hcy.

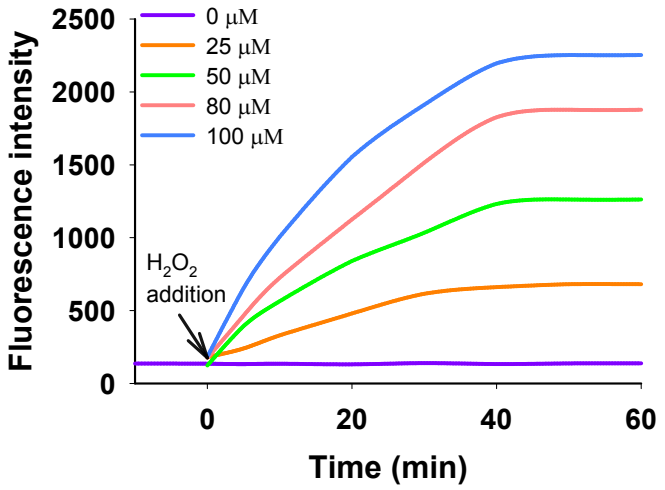

Figure S13. Time-dependent fluorescence changes of Mito-NIRHV (10 μM) toward H_2O_2 (0, 25, 50, 80 and 100 μM). The measurements were performed in DMSO/PBS, 3:7 (v/v), pH 7.4, at room temperature.

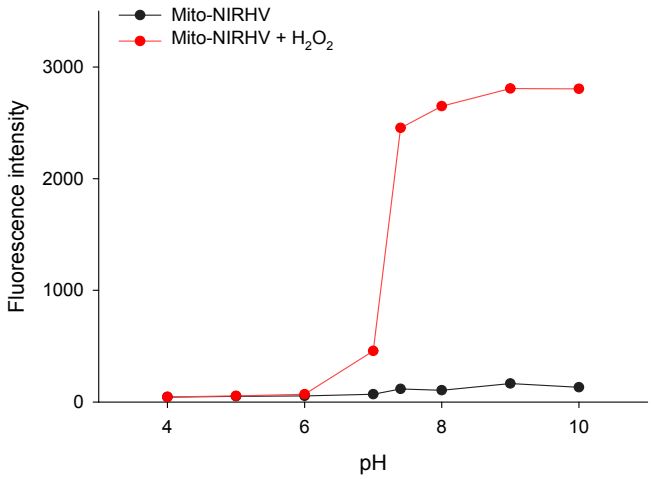

Figure S14. Effect of pH on the fluorescence of Mito-NIRHV (10 μM) in the absence and presence of H_2O_2 (100.0 μM). λ_{ex} / λ_{em} = 440 /700 nm.

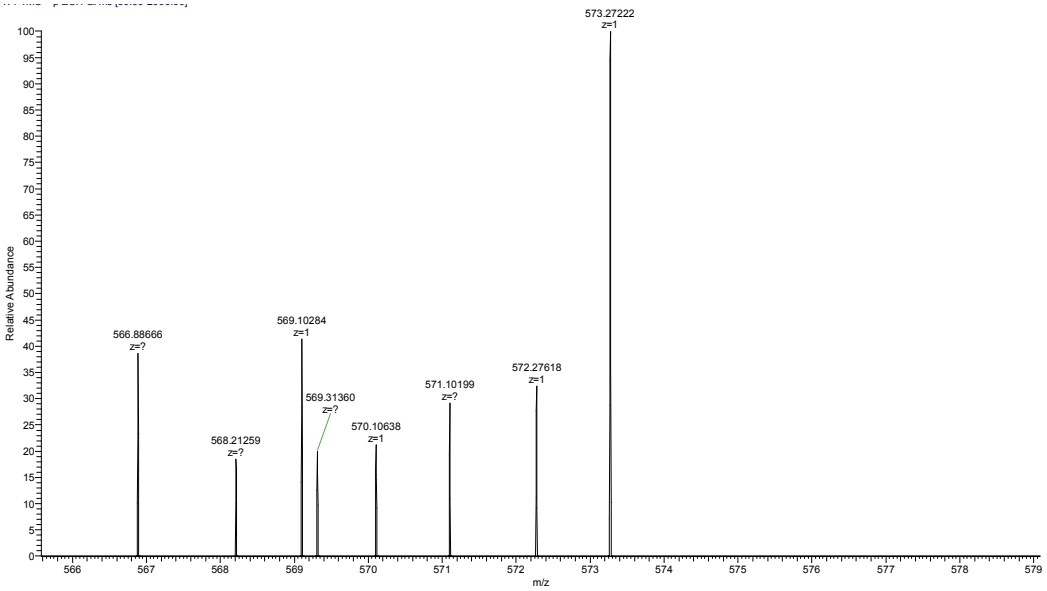

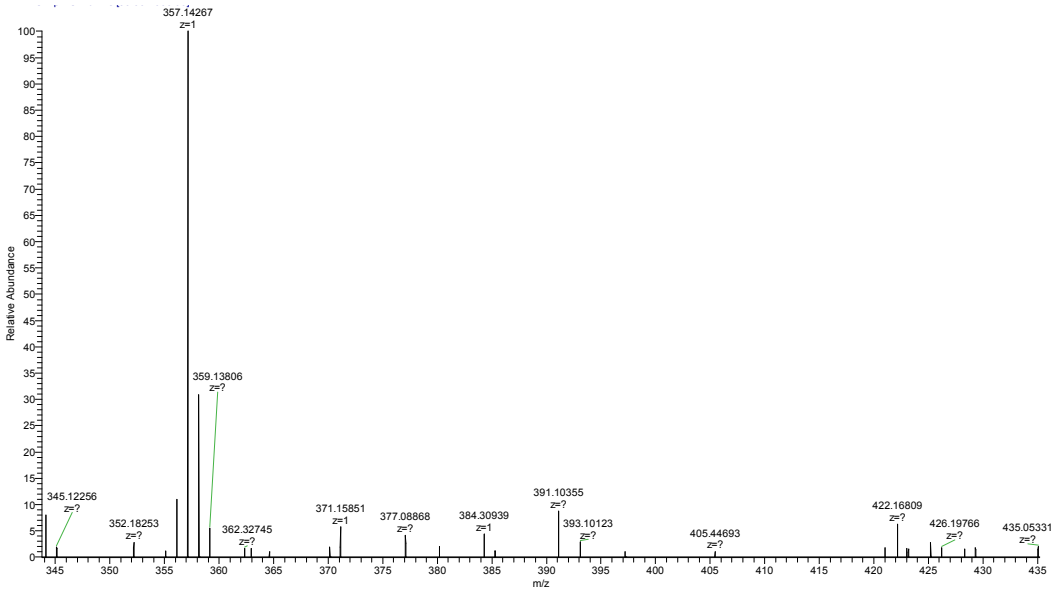

Figure S15. HRMS spectrum of Mito-NIRHV without (m/z 573.2722) and with H_2O_2 (m/z 357.1427).

Response of Mito-NIRHV to Viscosity

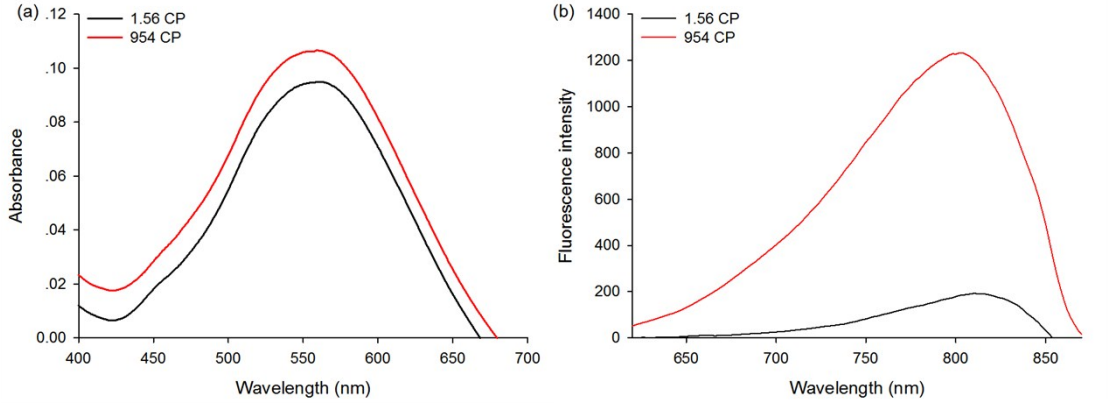

Figure S16. (a) Absorption and (b) fluorescence spectra of Mito-NIRHV (10 μM) in the solvent of low viscosity (black line) and high viscosity (red line).

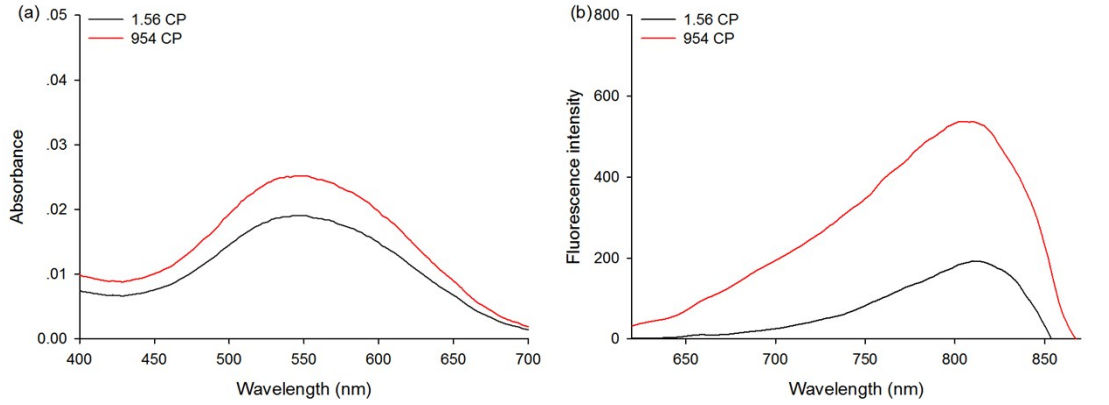

Figure S17. (a) Absorption and (b) fluorescence spectra of Mito-NIRHV (2 μM) in the solvent of low viscosity (black line) and high viscosity (red line).

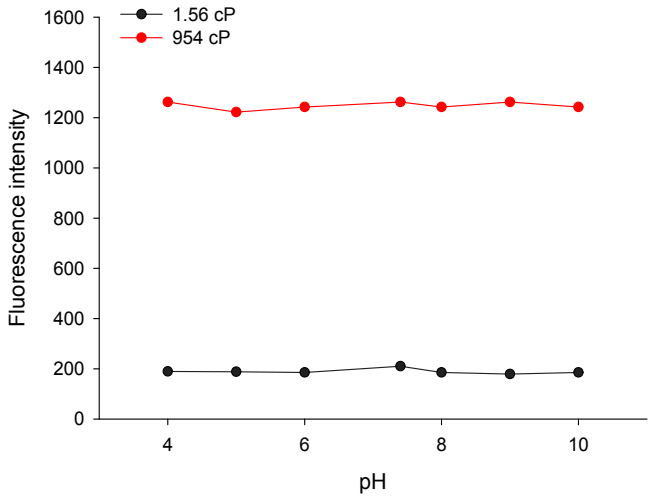

Figure S18. Effect of pH on the fluorescence of Mito-NIRHV (10 μM) at low and high viscosity. λ_{ex} / λ_{em} = 570 /800 nm.

Cell viability

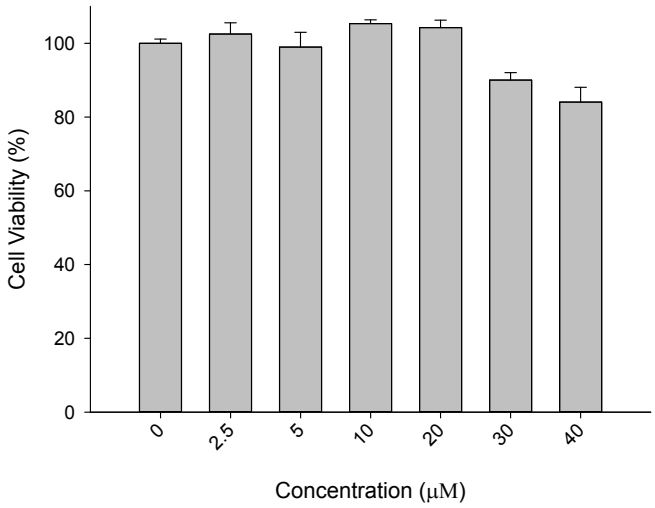

Figure S19. Cell viability values (%) estimated by MTT proliferation test versus concentrations of Mito-NIRHV. HeLa cells were cultured in the presence of 0-40 μM Mito-NIRHV.

Fluorescence Imaging in Living Cells

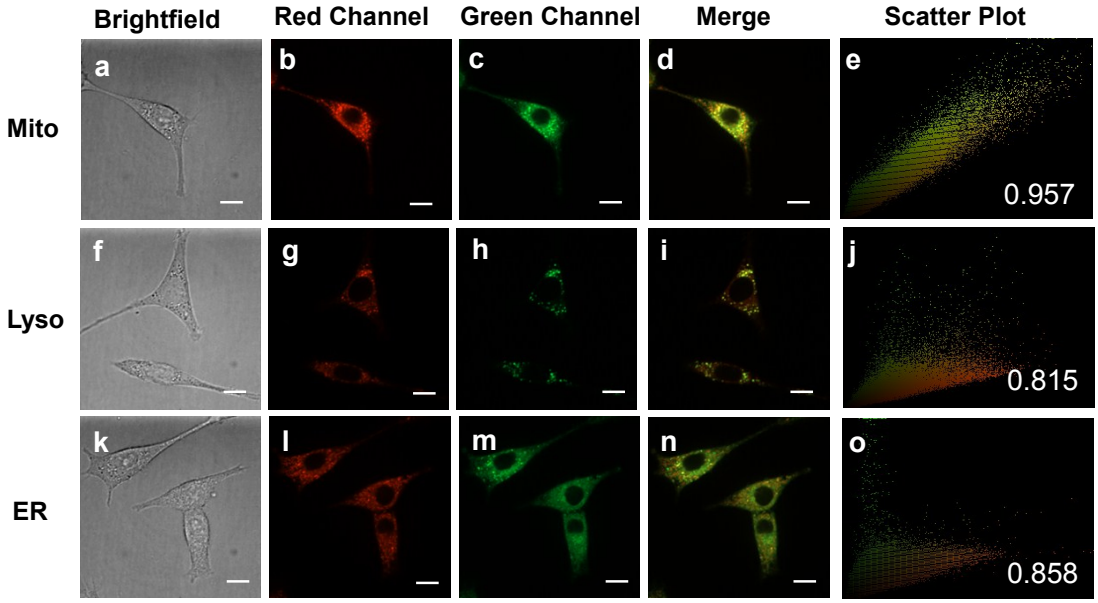

Figure S20. CLSM images of HeLa cells co-labeled with (a-d) Mito-NIRHV (10 μM) (pre-treated with 50 μM H_2O_2 for 1 h) /MitoTracker (500 nM), and (f−i) Mito-NIRHV (10 μM) (pre-treated with 50 μM H_2O_2 for 1 h) / LysoTracker (1 μM) at 37 °C. (k−m) Mito-NIRHV (10 μM) (pre-treated with 50 μM H_2O_2 for 1 h) / ER Tracker (1 μM) at 37 °C. (a, f, k) the brightfield image; (b, g, l) Red channel: 697 ± 29 nm for Mito-NIRHV, λ_{ex} = 488 nm; (c, h, m) green channel: 525 ± 25 nm for MitoTracker / LysoTracker or ER Tracker, λ_{ex} = 488 nm; and (d, i, n) the overlay images of red and green channels. (e, j, o) The correlation of Mito/Lyso/ER Tracker and Mito-NIRHV intensities. Scale bar = 10 μm.

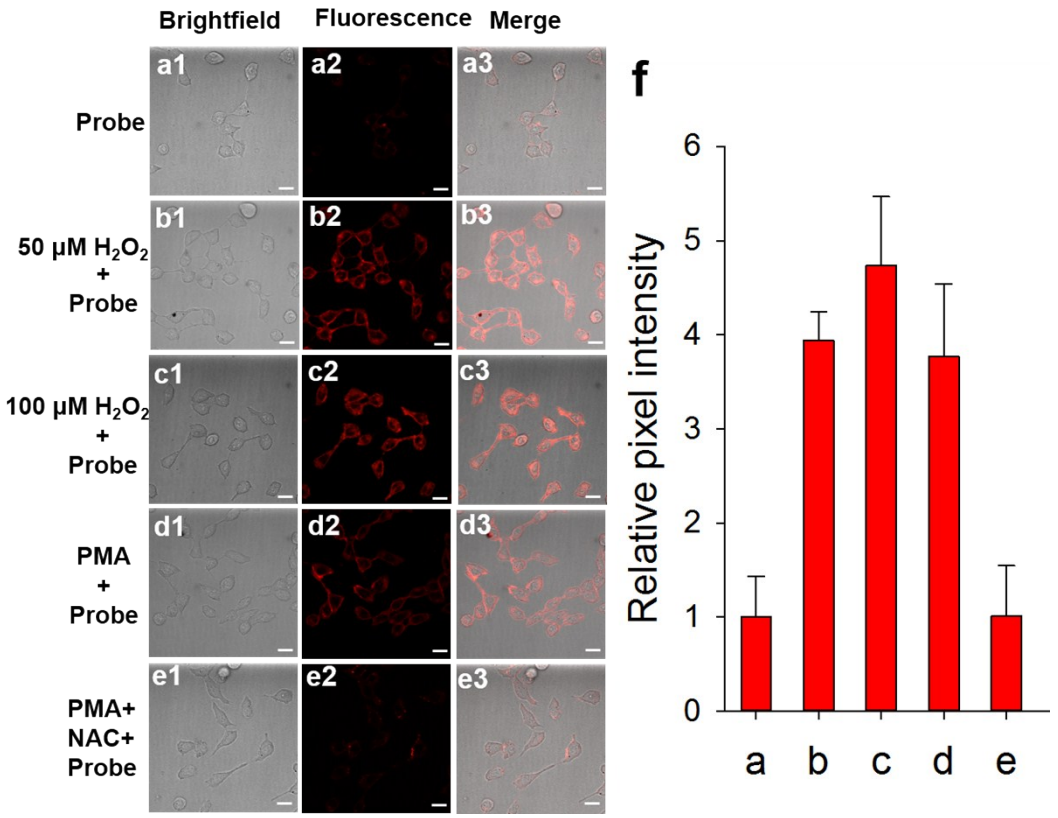

Figure S21. Fluorescence imaging of H_2O_2 in HeLa cells. (a) HeLa cells were only loaded with Mito-NIRHV (10 μM, 30 min). (b) HeLa cells were incubated with H_2O_2 (50 μM, 30 min), and then incubated with Mito-NIRHV (10 μM, 30 min). (c) HeLa cells were incubated with H_2O_2 (100 μM, 30 min), and then incubated with Mito-NIRHV (10 μM, 30 min). (d) HeLa cells were incubated with PMA (1 μg/mL, 30 min), and then incubated with Mito-NIRHV (10 μM, 30 min). (e) HeLa cells were successively incubated with PMA (1 μg/mL, 30 min), NAC (1 mM, 1 h), and Mito-NIRHV (10 μM, 30 min). (f) Relative fluorescence intensities of (a)−(e). λ_{ex} = 488 nm, λ_{em} = 668-726 nm. Scale bar: 20 μm.

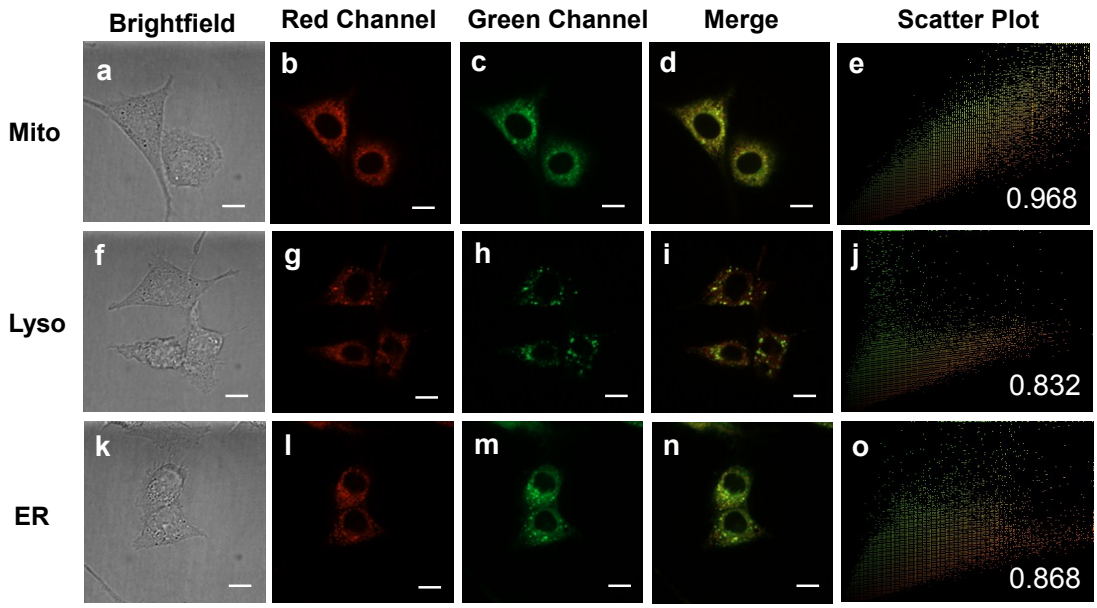

Figure S22. CLSM images of HeLa cells co-labeled with (a-d) Mito-NIRHV (10 μM) (pre-treated with 10 μM nystatin for 30 min) /MitoTracker (500 nM), and (f−i) Mito-NIRHV (10 μM) (pre-treated with 10 μM nystatin for 30 min) / LysoTracker (1 μM) at 37 °C. (k−m) Mito-NIRHV (10 μM) (pre-treated with 10 μM nystatin for 30 min) / ER Tracker (1 μM) at 37 °C. (a, f, k) the brightfield image; (b, g, l) Red channel: 785 ± 31 nm for Mito-NIRHV, λ_{ex} = 561 nm; (c, h, m) green channel: 525 ± 25 nm for MitoTracker / LysoTracker or ER Tracker, λ_{ex} = 488 nm; and (d, i, n) the overlay images of red and green channels. (e, j, o) The correlation of Mito/Lyso/ER Tracker and Mito-NIRHV intensities. Scale bar = 10 μm.

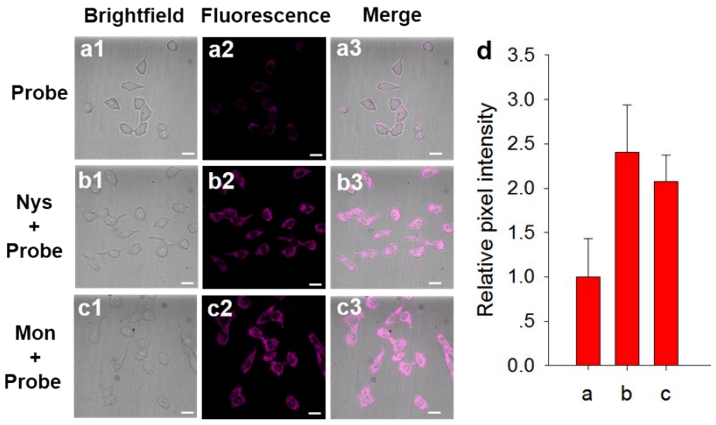

Figure S23. Fluorescence imaging of viscosity in HeLa cells. (a) HeLa cells were only loaded with Mito-NIRHV (10 μM, 30 min). (b) HeLa cells were incubated with nystatin (10 μM, 30min) and then incubated with Mito-NIRHV (10 μM, 30 min). (c) HeLa cells were incubated with monensin (10 μM, 30min) and then incubated with Mito-NIRHV (10 μM, 30 min). (d) Relative fluorescence intensities of (a)−(c). λ_{ex} = 561 nm, λ_{em} = 754-816 nm. Scale bar: 20 μm.

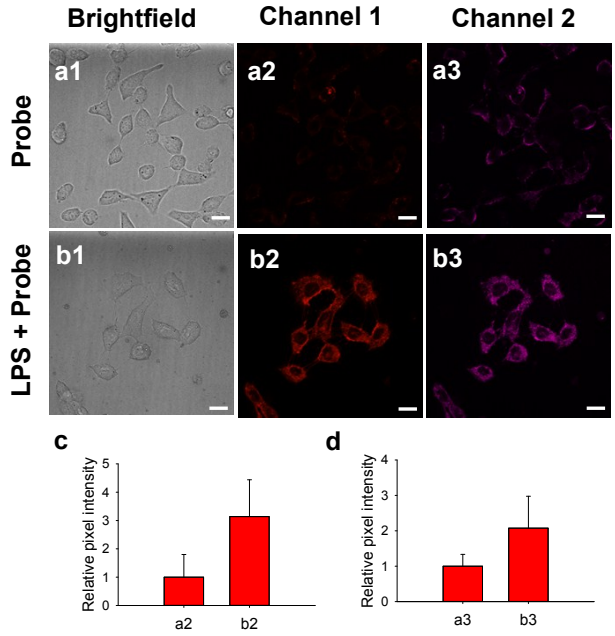

Figure S24. Fluorescence imaging of H_2O_2 and viscosity in HeLa cells. (a) HeLa cells were incubated with Mito-NIRHV (10 μM, 30 min). (b) HeLa cells were pretreated by LPS (100 μg/mL, 60 min), subsequently incubated with Mito-NIRHV (10 μM, 30 min). (c) Relative fluorescence intensities of (a2), (b2). (d) Relative fluorescence intensities of (a3), (b3). Channel 1: λex = 488 nm, λem = 668-726 nm; Channel 2: λex = 561 nm, λem = 754-816 nm. Scale bar: 20 μm.

Fluorescence Imaging in Living Mice

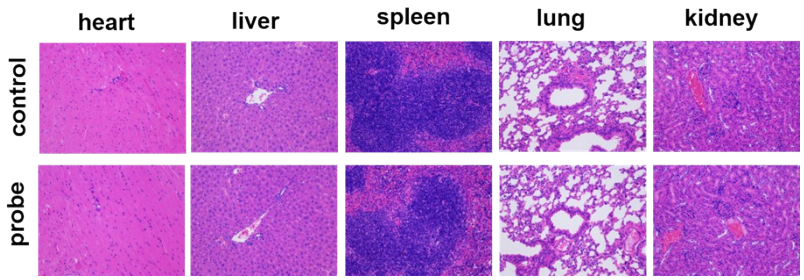

Figure S25. H&E staining results of organ sections (heart, liver, spleen, lung and kidney) collected from the control group and Mito-NIRHV (2 mg kg^{-1}) treated group.

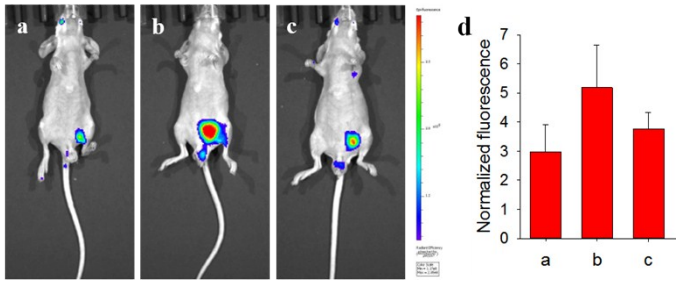

Figure S26. Fluorescence imaging of H_2O_2 in BALB/c mice. (a) Only Mito-NIRHV (1 mM, 100 μL) was injected as control. (b) Mouse pretreated with H_2O_2 (1 mM, 100 μL) for 30 min and then injected with Mito-NIRHV. (c) Mouse pretreated with rotenone for 1 h and then injected with Mito-NIRHV. (d) Relative fluorescence intensities of (a)−(c). The excitation filter was 430 nm, and the emission filter was 700 nm.

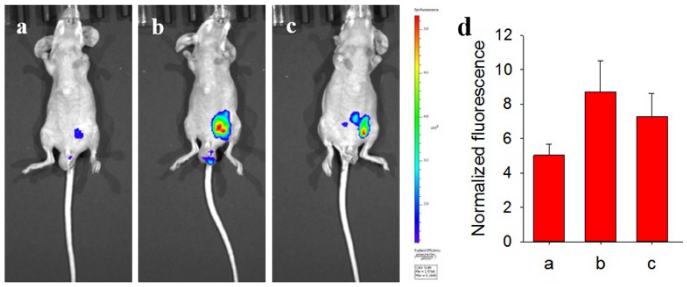

Figure S27. Fluorescence imaging of viscosity in BALB/c mice. (a) Only Mito-NIRHV (1 mM, 100 μL) was injected as control. (b) Mouse pretreated with nystatin for 4 h and then injected with Mito-NIRHV. (c) Mouse pretreated with monensin for 4 h and then injected with Mito-NIRHV. (d) Relative fluorescence intensities of (a)−(c). The excitation filter was 570 nm, and the emission filter was 800 nm.

Simultaneous Imaging of H_2O_2 and Viscosity in the Brain of the APP/PS1 Transgenic Mouse Model of AD

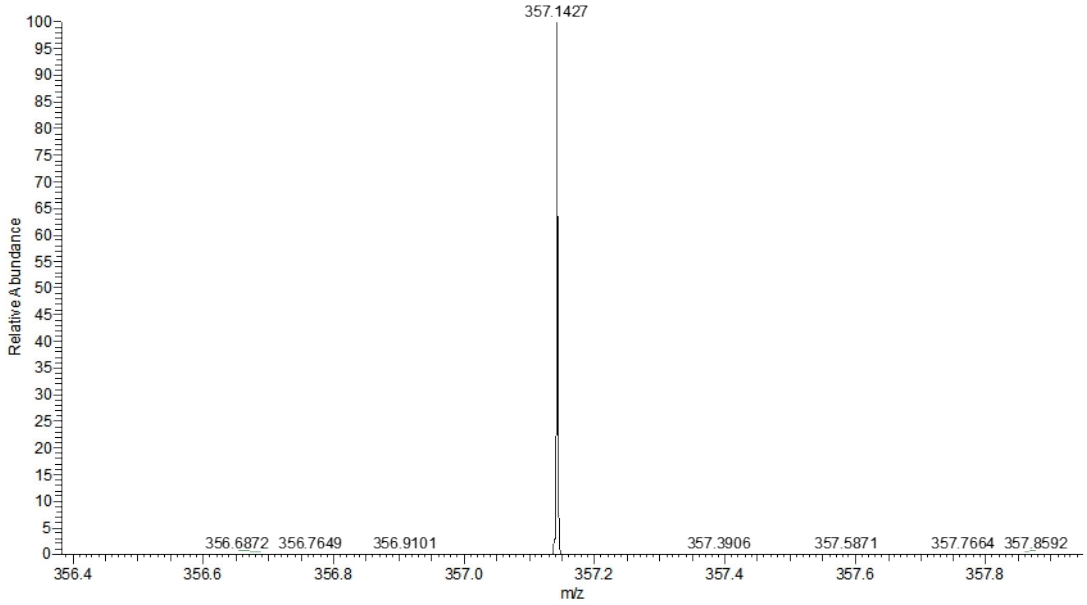

Figure S28. HRMS spectrum of Mito-NIRHV in brain extract.

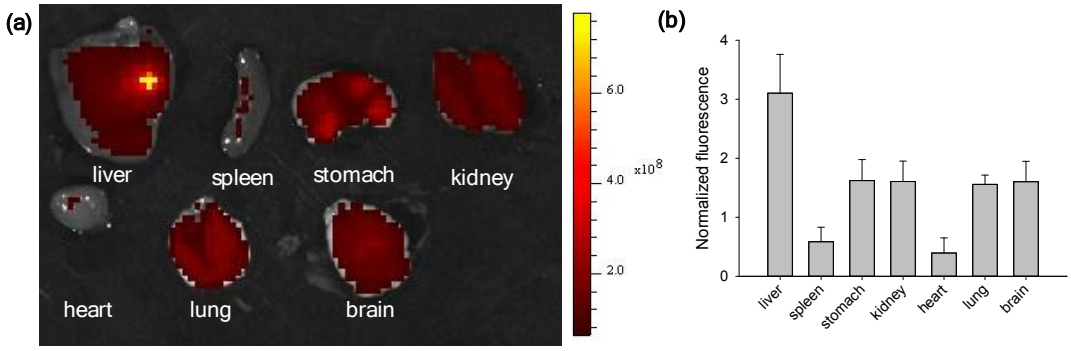

Figure S29. (a) Ex vivo fluorescence imaging of various organs from mice injected with Mito-NIRHV (2.0 mg/kg, 30% DMSO and 70% PBS). The mice were sacrificed at 1 h postinjection. (b) Quantitative results of fluorescence intensity for the ex vivo images of different organs. λ_{ex} = 430 nm, λ_{em} = 700 nm.

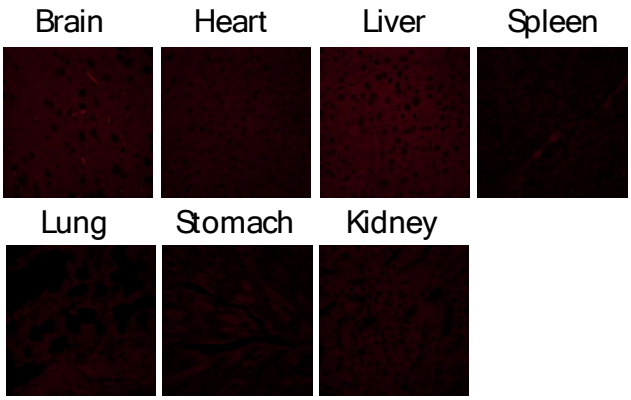

Figure S30. Fluorescence images of tissues of different mouse organs 1h after the i.v. injection of Mito-NIRHV (2.0 mg/kg in 30% DMSO and 70% PBS). λ_{ex} = 488 nm, λ_{em} = 700 nm.